Experimental implementation of Hardy-like quantum pigeonhole paradoxes

Shihao Ru,[1] Cen-Xiao Huang,[2,3] Xiao-Min Hu,[2,3] Chao Zhang,[2,3] Feiran Wang,[1,4] Ni Liu,[5,6] Weidong Tang,[5,*] Pei Zhang,[1,†] Bi-Heng Liu,[2,3,‡] and Fuli Li[1,§]

[1]*Ministry of Education Key Laboratory for Non-equilibrium Synthesis and Modulation of Condensed Matter, Shaanxi Key Laboratory of Quantum Information and Quantum Optoelectronic Devices, School of Physics of Xi'an Jiaotong University, Xi'an 710049, China*

[2]*CAS Key Laboratory of Quantum Information, University of Science and Technology of China, Hefei 230026, China*

[3]*CAS Center For Excellence in Quantum Information and Quantum Physics, University of Science and Technology of China, Hefei 230026, China*

[4]*School of Science of Xi'an Polytechnic University, Xi'an 710048, China*

[5]*School of Mathematics and Statistics, Shaanxi Normal University, Xi'an 710119, China*

[6]*Yulin Gaoxin No. 2 Middle School, Yulin 719000, China*

(Received 7 July 2022; accepted 27 January 2023; published 9 February 2023)

The general Hardy-like quantum pigeonhole paradoxes for n-qubit states were presented by Tang [W. Tang, Phys. Rev. A **105**, 032457 (2022)]. It has been shown that each of such paradoxes can be associated with an uncolorable solution of a specific vertex-coloring problem induced from the projected-coloring graph (a kind of unconventional graph). The Hardy-like quantum pigeonhole paradoxes can even give rise to a higher success probability in demonstrating the conflict between quantum mechanics and local or noncontextual realism than the previous Hardy's paradoxes. Moreover, multiqubit states and high-dimensional states can exhibit paradoxes. In contrast to only one type of contradiction presented in the original quantum pigeonhole paradox, we discussed two kinds of three-qubit projected-coloring graph states as the minimal illustration in our work. An optical experiment to verify such a stronger paradox is performed. This quantum paradox provides innovative thoughts and methods for exploring new types of stronger multiparty quantum nonlocality. It may have potential applications in untrusted multiparty communications and device-independent random number generation.

DOI: 10.1103/PhysRevA.107.022207

I. INTRODUCTION

Nowadays, the use of quantum approaches to solve some classical problems has attracted widespread attention. A succession of newly developed quantum technologies reveals their power for some specific tasks, such as quantum network [1–3], fault-tolerant quantum computation [4,5], and quantum metrology [6]. Based on the definite quantum feature, experts even proposed some quantum resource theories [7–10]. Quantum nonlocality [11–15] and contextuality [16–21] are two kinds of significant quantum resources. Not only do they play a pivotal role in many quantum technologies, but they may also produce many counterintuitive phenomena that may deepen our understanding of nature. For example, the original quantum pigeonhole paradox [22–26], as a paradigmatic consequence of quantum nonlocality or contextuality [27], presents a counterintuitive phenomenon: in a particular pre- and postselection procedure [28,29], if three particles (dubbed as three "quantum pigeons") are put into two boxes, then any pair of particles cannot stay in the same box, causing a violation to the classical pigeonhole counting principle [23].

Furthermore, quantum features can be visually exhibited by some specific mathematical structures, including graphs [30,31], braids [32], and knots [33], as well as some newly defined geometric and topological objects [34,35]. Performing coloring or sorting operations on such structures is the usual method to investigate the expected nonclassical features. To finish such a task, generally, the main challenge resides in accurately mapping the systems to the correlated mathematical objects and making a suitable rule compatible with all the quantum relations, but incompatible with at least one classical restriction. A well-known example, the graphical proof of the Kochen-Specker theorem [36–38] by the failure of noncontextuality (assigning values 0 or 1 to a set of rays), can be converted to a special coloring problem associated with the vertices of the induced orthogonal graph. Any pair of vertices connected with an edge indicates a mutually orthogonal relationship of the correlated rays. In addition, we note that only some special graphs can be regarded as orthogonal graphs.

Recently, a special counterintuitive mathematical object, the projected-coloring graph (PCG), was presented in Ref. [39]. The uncolorable PCGs can exhibit nonclassical quantum features. In other words, such uncolorable objects can only be simulated in some quantum processing rather than in the classical scenario. The minimal example of the uncolorable PCG can be considered to be another Penrose triangle description [40]. Moreover, the purpose of introducing this mathematical object is to offer a more intuitive understanding of a new kind of quantum pigeonhole paradox called the

*wdtang@snnu.edu.cn
†zhangpei@mail.ustc.edu.cn
‡bhliu@ustc.edu.cn
§flli@mail.xjtu.edu.cn

"Hardy-like quantum pigeonhole paradox." Since the coloring problem in the PCGs belongs to a topological problem and the (Hardy-like) quantum pigeonhole paradox is usually described in an algebraic framework, one can consider the former as a representation of the latter. The Hardy-like quantum pigeonhole paradox exhibits the nonclassical counting principle resorting to a Hardy-like argument [41–43]. Hardy's proof is arguably considered "one of the strangest and most beautiful gems yet to be found in the extraordinary soil of quantum mechanics" [44]. In addition, the Hardy-like paradoxes may have applications in device-independent random number generation [45,46].

In this work, we first introduce the Hardy-like quantum pigeonhole paradox, then show how to relate it to a classical vertex-coloring problem of a kind of unconventional graph, the projected-coloring graph. Here we realize a minimal experimental demonstration of this strong nonclassical feature by a heralded entanglement source of three entangled photons. Compared with Ref. [42], the demonstration of such Hardy-like quantum pigeonhole paradoxes does not require sophisticated techniques and is easier to implement. This quantum paradox provides a valuable tool to explore some new features of quantum mechanics. It also has practical applications in specific quantum information protocols, such as multiparty quantum communication tasks.

II. THEORETICAL DESCRIPTION OF HARDY-LIKE QUANTUM PIGEONHOLE PARADOX

We organized the theoretical part as follows. In Sec. II A, we first introduce the simplest Hardy-like quantum pigeonhole paradoxes, based on two three-qubit states and originally presented in Ref. [39]. The generation of these two states and the verification of the paradoxes are discussed in the next section. In Secs. II B and II C, we summarize the general Hardy-like pigeonhole paradoxes and introduce the related graph projected-coloring problems according to Ref. [39]. For a better understanding, we enumerate three kinds of quantum states for this paradox in Appendix B, including two kinds of general n-qubit states and one kind of n-qudit state. Furthermore, a different version of the Hardy-like quantum pigeonhole paradox, the quantum magic paradox, is presented in Appendix C.

A. The simplest Hardy-like quantum pigeonhole paradox

We denote the usual Pauli matrix σ_x (σ_y, σ_z) of the ith qubit by X_i (Y_i, Z_i), and let $|0\rangle_i$, $|1\rangle_i$ be two eigenstates of Z_i associated with eigenvalues $+1$, -1, respectively. Analogous to the conventional quantum pigeonhole paradox, the simplest system to show the Hardy-like quantum pigeonhole paradox requires three qubits [39], and the corresponding quantum state can be chosen as

$$|S\rangle = \tfrac{1}{2}(|000\rangle - |011\rangle - |101\rangle - |110\rangle), \tag{1a}$$

$$|S'\rangle = \tfrac{1}{2}(|000\rangle + |011\rangle + |101\rangle - |110\rangle). \tag{1b}$$

The state $|S\rangle = (|\circlearrowleft\circlearrowleft\circlearrowleft\rangle + |\circlearrowright\circlearrowright\circlearrowright\rangle)/\sqrt{2}$ is a special Greenberger-Horne-Zeilinger (GHZ) state, where $|\circlearrowleft\rangle = (|0\rangle + i|1\rangle)/\sqrt{2}$ and $|\circlearrowright\rangle = (|0\rangle - i|1\rangle)/\sqrt{2}$). We discuss state $|S\rangle$ in this section and state $|S'\rangle$ in Appendix A. Note that if the ith qubit is measured and found in $|0\rangle$, the other two must be in the eigenstate of X_jX_k with eigenvalue -1. Therefore, one can get the following quantum predictions:

$$P(X_2X_3 = -1|Z_1 = +1) = 1, \tag{2a}$$

$$P(X_1X_3 = -1|Z_2 = +1) = 1, \tag{2b}$$

$$P(X_1X_2 = -1|Z_3 = +1) = 1, \tag{2c}$$

$$P(Z_1 = Z_2 = Z_3 = +1) = \tfrac{1}{4} > 0. \tag{2d}$$

Here, $P(X_jX_k = -1|Z_i = +1) = 1$ denotes the conditional probability that X_j and X_k are measured with outcomes satisfying $X_jX_k = -1$ given the result of $Z_i = 1$. $P(Z_1 = Z_2 = Z_3 = +1)$ is the joint probability of obtaining $Z_1 = 1, Z_2 = 1, Z_3 = 1$.

Consider a run of the experiment in which Z_1, Z_2, Z_3 are measured and the results $Z_1 = 1, Z_2 = 1, Z_3 = 1$ are obtained (the corresponding probability is $1/4$). We assume that the state $|S\rangle$ can be modeled by a local realistic description. Since $Z_1 = 1$ is obtained in this run of the experiment, according to Eq. (2a), if X_2 and X_3 were measured in this run, their results should satisfy $X_2X_3 = -1$, indicting that qubits 2 and 3 ("pigeons") cannot stay in the same state ("box"). Likewise, from Eq. (2b) and Eq. (2c), we can infer that qubits 1 and 3, and qubits 1 and 2, cannot stay in the same box either, contradicting the classical pigeonhole principle. We get a three-qubit Hardy-like quantum pigeonhole paradox.

In addition, we can understand this paradox from the angle of the conventional Hardy's paradox based on the constraint $(I - X_2X_3)(I - X_1X_3)(I - X_1X_2)/8 = 0$ as well. Similar to the standard construction of the Hardy's paradox presented in Ref. [14], we can get a three-qubit common Hardy's paradox by invoking four extra constraints: $P(\frac{I-X_2X_3}{2} = 1|Z_1 = +1) = 1, P(\frac{I-X_1X_3}{2} = 1|Z_2 = +1) = 1, P(\frac{I-X_1X_2}{2} = 1|Z_3 = +1) = 1$, and $P(Z_1 = Z_2 = Z_3 = +1) = 1/4$. We stress that these constraints are more general, in contrast to Eqs. (2a)–(2d), since in the aforementioned argument of the Hardy-like pigeonhole paradox we adopted a stronger realistic assumption. This replaces $(X_iX_j)(\lambda)$ with $X_i(\lambda)X_j(\lambda)$, thus requiring the classical pigeonhole principle. In view of this, the Hardy-like pigeonhole paradox is just a weaker version of the Hardy's paradox. A detailed discussion is in Appendix D.

Notice that in the above argument, we only discuss the contradiction arising from the case in which Z_1, Z_2, Z_3 are measured with the results $Z_1 = 1, Z_2 = 1, Z_3 = 1$. In fact, by introducing other conditional probability constraints and considering other results such as $Z_1 = 1, Z_2 = -1, Z_3 = -1$, three more similar paradoxes can be constructed. Namely, sometimes a given quantum state may induce more than one Hardy-like quantum pigeonhole paradox. But to simplify, here we only discuss the paradox arising from the constraint given by the joint probability that all the involved Z_i are measured with outcomes of $+1$.

B. General Hardy-like quantum pigeonhole paradoxes

The general Hardy-like quantum pigeonhole paradoxes can be constructed based on a special kind of state called PCG

states. The n-qubit PCG state can be defined as

$$|P_n\rangle = \frac{1}{\sqrt{p+1}}\left(|00\cdots0\rangle - \sum_{i\in\mathcal{I}} \theta_i |\vec{0}\rangle_{\overline{\mathcal{S}}_i} |\vec{1}\rangle_{\mathcal{S}_i}\right), \tag{3}$$

where $\mathcal{S}_i \subset \mathcal{N}$, $\overline{\mathcal{S}}_i = \mathcal{N} - \mathcal{S}_i$ and $\mathcal{N} = \{1, 2, \ldots, n\}$. The size of $\mathcal{S}_i$ satisfies $2 \leqslant |\mathcal{S}_i| < n$ and $|\mathcal{S}_i \cup \mathcal{S}_j| > \max\{|\mathcal{S}_i|, |\mathcal{S}_j|\}$ $(i \neq j)$. In addition, $|\vec{0}\rangle_{\mathcal{S}_i} \equiv \otimes_{k\in\mathcal{S}_i}|0\rangle_k$, $|\vec{1}\rangle_{\mathcal{S}_i} \equiv \otimes_{k\in\overline{\mathcal{S}}_i}|1\rangle_k$, $\theta_i = \pm 1$, and $p = \sum_{i\in\mathcal{I}} |\theta_{\mathcal{S}_i}|$. $\mathcal{I}$ is an index set, which is used for labeling a group of specific subsets of $\mathcal{N}$. If the qubits in $\overline{\mathcal{S}}_i$ are measured and found in $|\vec{0}\rangle_{\overline{\mathcal{S}}_i}$, then the others are found in the eigenstate of $\prod_{k\in\mathcal{S}_i} X_k$ with eigenvalue θ_i. Some tools are useful in the argument of Hardy-like quantum pigeonhole paradoxes. First, a Hardy matrix A with respect to a PCG state $|P_n\rangle$ can be defined as $A = (A_{ij})_{|\mathcal{I}|\times n}$ with elements $A_{ij} = 1$ if $i \in \mathcal{I}$ and $j \in \mathcal{S}_i$, and $A_{ij} = 0$ otherwise. Next, an augmented Hardy matrix B is defined by a dilated matrix $B = (A|\vec{\Theta})$, where the ith element of the $|\mathcal{I}|$ vector $\vec{\Theta}$ is $\Theta_i = (\theta_{\mathcal{S}_i} + |\theta_{\mathcal{S}_i}|)/2$. Then we can classify the PCG states into two families: (1) $\mathrm{rank}(A) = \mathrm{rank}(B)$ and (2) $\mathrm{rank}(A) \neq \mathrm{rank}(B)$.

For a state $|P_n\rangle$ in the form of Eq. (3) and satisfying $\mathrm{rank}(A) \neq \mathrm{rank}(B)$, we can get the following conditions:

$$\prod_{k\in\mathcal{S}_i} X_k = -\theta_i, \quad (i \in \mathcal{I})$$
$$\text{if } Z_{j_1} = Z_{j_2} = \cdots = Z_{j_{n-|\mathcal{S}_i|}} = 1, \tag{4}$$

where $j_1, j_2, \ldots, j_{n-|\mathcal{S}_i|} \in \overline{\mathcal{S}}_i$, and $Z_{j_l} = 1$ $(l \in \{1, 2, \ldots, n\})$ denotes an event of measuring Z_{j_l} with an outcome of $+1$, and likewise $\prod_{k\in\mathcal{S}_i} X_k = -\theta_i$. Equations (4) have a total of $|\mathcal{I}|$ items. In addition, it has the following quantum prediction as well:

$$P(Z_1 = Z_2 = \cdots = Z_n = 1) = \frac{1}{p+1} > 0. \tag{5}$$

The relationship $\mathrm{rank}(A) \neq \mathrm{rank}(B)$ will cause $\prod_{k\in\mathcal{S}_i} X_k = -\theta_i$ $(i \in \mathcal{I})$ cannot be satisfied simultaneously by any local hidden variable or noncontextual hidden variable models [39]. Then the classical pigeonhole counting principle is broken, i.e., one gets an n-qubit Hardy-like quantum pigeonhole paradox. Based on Eqs. (3)–(5), we have designed three general kinds of PCG states, i.e., two kinds of general n-qubit states and one kind of n-qudit state (see Appendix B), which show the n-qubit and n-qudit paradoxes, respectively.

C. Graph projected-coloring problems and beyond

In contrast to the lack of pictorial representations for a common Hardy's paradox, one can find some interesting representations for the Hardy-like quantum pigeonhole paradox by some mathematical objects (e.g., graphs) or problems.

First, we introduce a vertex-coloring problem [39] of an n-vertex PCG which can be associated with the n-qubit Hardy-like quantum pigeonhole paradox, i.e., an n-vertex PCG G to an n-qubit PCG state $|P_n\rangle$, where a n-vertex PCG can be defined as follows.

For any PCG state $|P_n\rangle$, a PCG G is defined as an unconventional graph consisting of a set of vertices $V = \{1, 2, \ldots, n\}$ and a set of weighted edges $E = \{\mathcal{S}_i | i = 1, 2, \ldots, p\}$. The weights of the edge $\mathcal{S}_i$ are colored as red (R) and green (G), and the corresponding coefficients $\theta_{\mathcal{S}_i}$ are equal to $+1$ and -1, respectively. In contrast to a usual graph, two or more (but less than n) vertices are allowed in an edge of an n-vertex PCG. Moreover, to guarantee that there are no subedges inside any edge in E, an extra constraint should be imposed, namely, for any two edges $\mathcal{S}_i$ and $\mathcal{S}_j$, $|\mathcal{S}_i \cup \mathcal{S}_j| > \max\{|\mathcal{S}_i|, |\mathcal{S}_j|\}$. Then the rule of graph projected-coloring problem can be described as follows:

(1) Each vertex $v_i \in V$ must be colored with either R or G; the coloring value $C(v_i)$ of a vertex v_i is defined as $C(v_i) = -1$ if the vertex v_i is colored with red, and $C(v_i) = +1$ otherwise.

(2) The coloring value $C(\mathcal{S}_i)$ of an edge $\mathcal{S}_i$ can be defined as $C(\mathcal{S}_i) = -1$ if the related weight is R, and $C(\mathcal{S}_i) = +1$ otherwise.

(3) A PCG G is colorable if $\prod_{v_i\in\mathcal{S}_i} C(v_i) = C(\mathcal{S}_i)$ holds for any edge $\mathcal{S}_i \in E$, otherwise uncolorable.

According to Ref. [39], any uncolorable PCG is associated with a proof of Hardy-like quantum pigeonhole paradox, which is related to a PCG state with $\mathrm{rank}(A) \neq \mathrm{rank}(B)$. Note that the uncolorable PCG is a different kind of impossible object, which cannot exist in the classical world. In fact, using impossible objects as analogies with some quantum features is not rare in the study of quantum theories, such as the Hilbert hotel [47] and Penrose square [48]. In this regard, another example of this paradigm can be considered, using the uncolorable PCG to illustrate the Hardy-like quantum pigeonhole paradox.

Take the case of three-vertex PCGs as an example. As shown in Fig. 1, there are seven types of three-vertex PCGs, where Figs. 1(a) and 1(b) are uncolorable PCGs, and the others are all colorable PCGs. Figures 1(a) and 1(b) show two three-qubit Hardy-like quantum pigeonhole paradoxes based on the state $|S\rangle$ and $|S'\rangle$, respectively. We experimentally measure the quantum feature based on these two states. In all, $|S\rangle$ and $|S'\rangle$ are two minimal states which can induce the Hardy-like quantum pigeonhole paradox. They are local unitary equivalent as well as in experimental realization, but reveal different two kinds of the Hardy-like quantum pigeonhole paradox. Moreover, in analogy to the hypergraph state [49], here the PCG states can be considered as a kind of generalized graph state as well.

Apart from the uncolorable PCG representation for the Hardy-like quantum pigeonhole paradox, we can find other representations for some special kinds of such paradoxes, e.g., the quantum map coloring representation [39]. Another interesting version of a kind of specific Hardy-like quantum pigeonhole paradox is the quantum magic square paradox (for more details, see Appendix C).

Compared with other versions of the Hardy's paradox, the Hardy-like quantum pigeonhole paradox has at least two advantages: (1) a simpler and more intuitive graphical representation (PCGs), and (2) sometimes a higher success probability to show the contradiction between quantum mechanics and local or noncontextual realism. For example, considering the Hardy-like quantum pigeonhole paradox based on the PCG state $|S_1(n)\rangle$ (Appendix B), we can find that the success probability is $1/(n+1)$. By contrast, in the

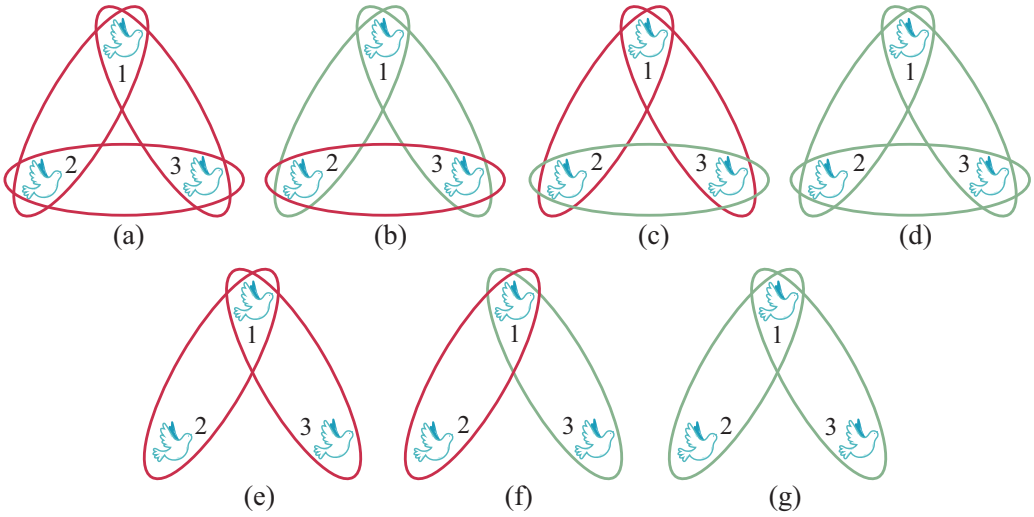

FIG. 1. The graph projected-coloring problem studies the colorability of vertices under the condition of given edge colors. There are seven categories of three-vertex PCGs, and the constraint relations of the edges in each category are equivalent. The qubits on any edge can be regarded as a postselected subsystem after projecting all the other qubits to the state $|0\rangle$. The color of this edge depends on the parity of the constraint which specifies the number of qubits staying in the box of $|+\rangle$. A red edge ($\{j,k\}$) visually shows the constraint relation of different colors between the vertices j and k. It means that any pair of the qubits cannot stay in the same box ($X_jX_k=-1$) if the other qubit is postselected to the state $|0\rangle$. And a green edge ($\{j,k\}$) visually shows the constraint relation of the same color between the vertices j and k. (a) The first type of three-qubit uncolorable PCGs, which contains only one PCG and corresponds to the PCG state $(|000\rangle-|011\rangle-|101\rangle-|110\rangle)/2$. Notice that three red edges imply a group of relations $X_1X_2=-1$, $X_2X_3=-1$, and $X_1X_3=-1$. One can find consistent solutions for each pair of them (from the classical perspective), but for all three of these relations, there are no globally inconsistent solutions. Such a group of relations seems like a Penrose triangle in which individually consistent corners (a pair of edges generate each corner) form a globally inconsistent structure. (b) A representative example of the second type of three-qubit uncolorable PCGs, which is associated with another one PCG state $(|000\rangle+|011\rangle+|101\rangle-|110\rangle)/2$. (c)–(g) Representative examples of all kinds of three-qubit colorable PCGs.

generalized n-qubit Hardy's paradox [42], this probability can only be $1/2^{n-1}$.

III. EXPERIMENT

A. Methods

Our experimental setup for generating the states $|S\rangle$ and $|S'\rangle$ is illustrated in Fig. 2. We first prepared two pairs of polarized-entangled photons in the $|\psi^-\rangle=(|H\rangle|V\rangle-|V\rangle|H\rangle)/\sqrt{2}$, in which $H(V)$ denotes $|0\rangle$ ($|1\rangle$) and the horizontal (vertical) polarization state of photons. We adopted type-II phase-match beamlike compound β-barium (c-BBO) crystals, with a 780-nm true-zero-order half-wave plate (HWP) inserted between BBOs, to obtain polarized-entangled photons.

Pumped by ultraviolet laser pulses, photons pairs in the same state $|H_e\rangle|V_o\rangle$ are generated through spontaneous parametric down conversion since two BBO crystals have the same cutting angle and are placed in the same manner. Here subscripts $o(e)$ indicate two spatial modes on which photons are ordinary (extraordinary) light. Passing the true-zero-order HWP at 45°, the state of photon pairs generated by the left BBO is converted to $|V_e\rangle|H_o\rangle$. By careful spatial and temporal compensations, polarized-entangled photons in the state $|\psi^-\rangle=(|H_e\rangle|V_o\rangle-|V_e\rangle|H_o\rangle)/\sqrt{2}$ are successfully prepared. More details about this sandwich-structure c-BBO for generating a polarized-entangled source are in Ref. [50]. In our experimental setup, pump pulses pass through two c-BBOs successively. In this way, two photon pairs are prepared in state,

$$|\Psi_1\rangle=\left(|H\rangle_{e_1}|V\rangle_{o_1}-|V\rangle_{e_1}|H\rangle_{o_1}\right)/\sqrt{2}\otimes\left(|H\rangle_{e_2}|V\rangle_{o_2}-|V\rangle_{e_2}|H\rangle_{o_2}\right)/\sqrt{2}, \quad (6)$$

with nonvanishing probability, in which subscripts 1 and 2 are used to distinguish the photons generated from which c-BBOs. Then by transforming the first photon pair to the Bell state $(|HH\rangle-|VV\rangle)/\sqrt{2}$ with a HWP at 45° for the e_1 mode photon, we obtain the state

$$|\Psi_2\rangle=\left(|H\rangle_{e_1}|H\rangle_{o_1}-|V\rangle_{e_1}|V\rangle_{o_1}\right)/\sqrt{2}\otimes\left(|H\rangle_{e_2}|V\rangle_{o_2}-|V\rangle_{e_2}|H\rangle_{o_2}\right)/\sqrt{2}. \quad (7)$$

The vertically polarized photon $|V\rangle_{o_2}$ is used as a trigger signal, and we use a HWP at 22.5° for the e_2 mode photon. Afterwards, the two photons in modes e_1 and e_2 are directly combined on a PBS. The PBS transmits H and reflects V, leading to a coincidence registration of a single photon at each output. In this way, the two terms $|H\rangle_{e_1}|H\rangle_{o_1}|H\rangle_{e_2}$ and $|V\rangle_{e_1}|V\rangle_{o_1}|V\rangle_{e_2}$ are postselected, i.e.,

$$|\Psi_3\rangle=\frac{1}{\sqrt{2}}\left(|H\rangle_{e_1}|H\rangle_{o_1}|H\rangle_{e_2}+|V\rangle_{e_1}|V\rangle_{o_1}|V\rangle_{e_2}\right). \quad (8)$$

In this step, to achieve great spatial and temporal overlap, a movable prime is used to guarantee the same delay between the two spatial modes e_1 and e_2. The corresponding Hong-Ou-Mandel interference is illustrated in Fig. 3. We add a QWP at 0° and a HWP at 22.5° in each mode e_1, e_2, and o_1 to rotate

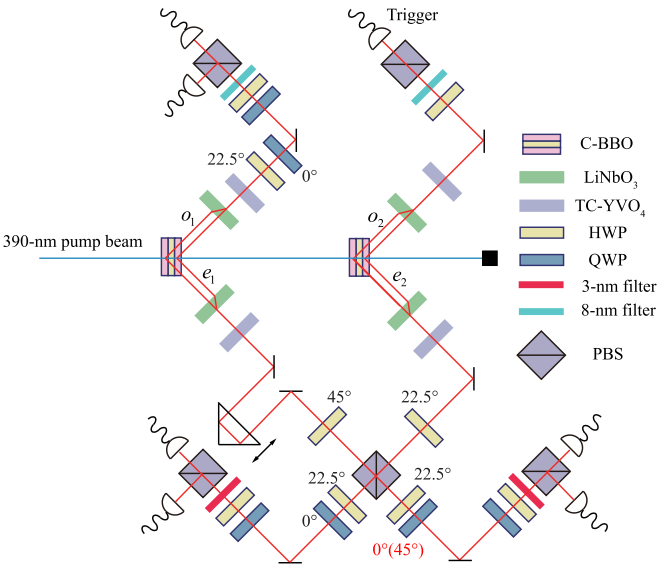

FIG. 2. Experimental setup. The pump beam, with a central wavelength of 390 nm, a duration of 140 fs, and a repetition rate of 76 MHz, passes through two c-BBO crystals successively to generate two pairs of polarized-entangled photons. Photons in spatial modes e_1 and e_2 overlap on PBS; a movable prime is used to guarantee that the temporal delay between two paths is equal. Photons in modes e_1 and e_2 are spectrally filtered with 3-nm bandwidth filters, and photons in modes o_1 and o_2 are spectrally filtered with 8-nm bandwidth filters for a better collection efficiency. We show that the relative phase exists for two states $|S\rangle$ and $|S'\rangle$, only changing one QWP's angle from 0° to 45° (red mark). c-BBO: compound β-barium borate crystal; $LiNbO_3$: $LiNbO_3$ crystal for spatial compensation; TC-YVO_4: YVO_4 crystal for temporal compensation; HWP: half-wave plate; QWP: quarter-wave plate; PBS: polarizing beam splitter.

the state $|\Psi_3\rangle$ to

$$|\Psi_4\rangle = \tfrac{1}{2}\big(|H\rangle_{e_1}|H\rangle_{o_1}|H\rangle_{e_2} - |H\rangle_{e_1}|V\rangle_{o_1}|V\rangle_{e_2} - |V\rangle_{e_1}|H\rangle_{o_1}|V\rangle_{e_2} - |V\rangle_{e_1}|V\rangle_{o_1}|H\rangle_{e_2}\big), \tag{9}$$

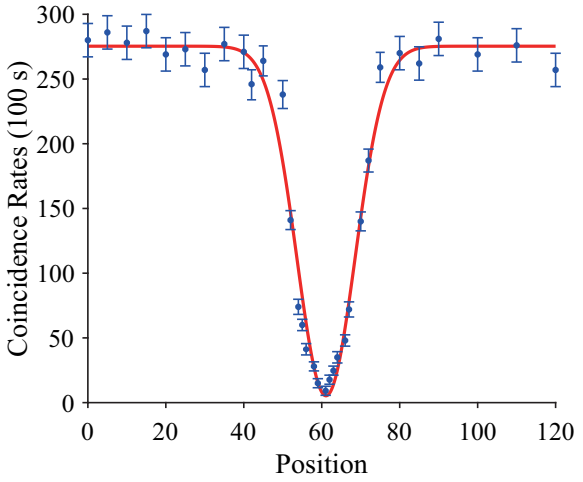

FIG. 3. The Hong-Ou-Mandel interference of our setup; its visibility is 0.962 ± 0.015.

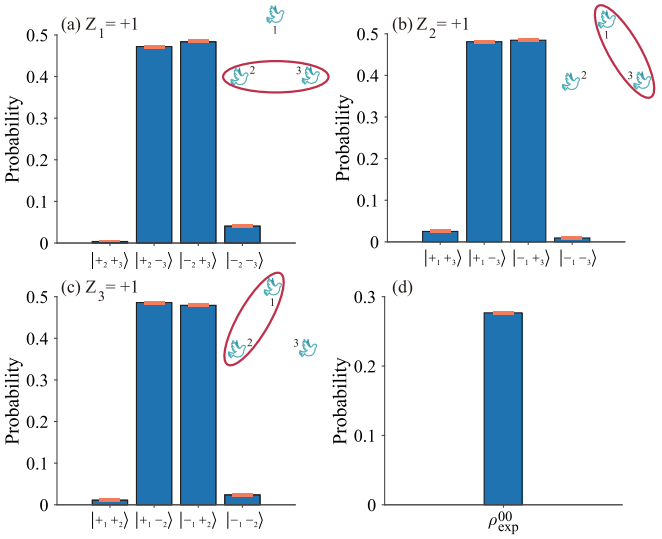

FIG. 4. Data show the quantum probabilities of measurements for the Hardy-like pigeonhole paradox on three-qubit state $|S\rangle$. (a) Experimental results for X_2X_3 if $Z_1 = +1$, (b) experimental results for X_1X_3 if $Z_2 = +1$, (c) experimental results for X_1X_2 if $Z_3 = +1$, (d) experimental results for $Z_1 = Z_2 = Z_3 = +1$. The error bars in both subplots correspond to 1σ standard deviation.

which is the state $|S\rangle$. Additionally, by only changing the QWP's angle from 0° to 45° (red mark), the state $|S'\rangle$ is prepared.

In our experiment, the fidelity $F = [\mathrm{Tr}(\sqrt{\sqrt{\rho_t}\rho_{\mathrm{exp}}\sqrt{\rho_t}})]^2 = 0.931 \pm 0.023$, where ρ_{exp} and $\rho_t = |S\rangle\langle S|$ are the experimental and theoretical density matrices, respectively. Here, the errors are calculated by assuming Poisson distribution for counting statistics, and resampling over recorded data. In addition, we observed genuine tripartite entanglement of state ρ_{exp} by the tripartite negativity [51],

$$N_{123}(\rho) = (N_{1,(23)}N_{2,(13)}N_{3,(12)})^{1/3}, \tag{10}$$

where the bipartite negativities are defined as $N_{I,(JK)} = -2\sum_i \sigma_i(\rho^{TI})$, with $\sigma_i(\rho^{TI})$ being the negative eigenvalues of ρ^{TI}. The partial transpose of ρ is with respect to subsystem I, $\langle i_I, j_{JK}|\rho^{TI}|k_I, l_{JK}\rangle = \langle k_I, l_{JK}|\rho|i_I, j_{JK}\rangle$ with $I = 1, 2, 3$ and $JK = 23, 13, 12$, respectively. We calculated the experimental value of the tripartite negativity, $N_{123}(\rho_{\mathrm{exp}}) = 0.974 \pm 0.013$, which is close to the theoretical value 0.9785 and clearly shows its genuine tripartite entanglement.

B. Experimental results of $|S\rangle$

As illustrated in Fig. 2, we can use this experiment setup to verify the above quantum feature of the minimal system. For the implementation of the three-qubit Hardy-like quantum pigeonhole paradox, we measured Eqs. (2a)–(2c) and (2d). All of these experimental results are shown in Fig. 4, where

$$\langle X_2X_3\rangle = -0.911 \pm 0.012 \text{ if } Z_1 = +1, \tag{11a}$$

$$\langle X_1X_3\rangle = -0.931 \pm 0.017 \text{ if } Z_2 = +1, \tag{11b}$$

$$\langle X_1X_2\rangle = -0.930 \pm 0.020 \text{ if } Z_3 = +1, \tag{11c}$$

and the probability of event $Z_1 = Z_2 = Z_3 = +1$ is

$$P(Z_1 = Z_2 = Z_3 = +1) = 0.277 \pm 0.009. \quad (12)$$

In any local hidden variable theories or noncontextual hidden variable theories, according to the classical pigeonhole principle, events $X_1X_2 = X_1X_3 = X_2X_3 = -1$ cannot jointly hold, which leads to a zero probability of obtaining $Z_1 = Z_2 = Z_3 = +1$. However, our experimental results show a probability of 0.277 ± 0.009 to get $Z_1 = Z_2 = Z_3 = +1$. Although not perfect, it is enough to exhibit the Hardy-type all-versus-nothing phenomenon and can successfully prove this nonclassical problem.

In fact, the paradox constructed from this state is a representative example corresponding to another kind of PCG (see Fig. 1). Moreover, it is known that there are only two types of Hardy-like quantum pigeonhole paradoxes for three-qubit systems. In this sense, we have completely verified this kind of quantum feature for the minimal systems. Only projection measurements of a polarization degree of freedom were performed in our experiment, and we did not introduce other auxiliary qubits. It differs from previous experiments that required weak measurements and additional resources. In addition, there are two main reasons for the imperfect experimental results. The first is the angle of all wave plates in the experiments. The HWP in c-BBO and compensation crystals affect the entangled source and the visibility of the four-photon Hong-Ou-Mandel interference result. All HWPs and QWPs used for projection measurements are manually adjusted, introducing corresponding experimental errors. The other is the stability of our optical setup. The raw experimental correlation counts were obtained from two nights (16 hours in total) of measurements, during which the pump laser power would be slightly reduced. All these factors caused the experimental results to deviate from the expected theoretical values.

IV. CONCLUSION AND DISCUSSION

In conclusion, with the general projected-coloring graph states, we have studied the general Hardy-like quantum pigeonhole paradoxes and used the graph projected-coloring problems to portray which coexisting postselections may lead to noncoexisting colorings. We experimentally verified this feature in the minimal three-qubit systems. Compared with the original quantum pigeonhole paradox, which needs some sophisticated skills such as weak measurement [25], the coloring problems (Hardy-like quantum pigeonhole paradoxes) are more feasible in the experimental implementation.

These quantum paradoxes can be considered as a kind of special many-particle Hardy paradox. One can use a special kind of graph called projected-coloring graphs to design other different paradoxes. There are more interesting problems that are a particular case of these graph coloring problems, such as the quantum magic square problems and quantum map coloring problems in Appendix C. Additionally, the Hardy-like quantum pigeonhole paradox is a powerful tool to study a kind of GHZ-like nonlocality unnoticed before. Unlike the common GHZ paradox, the proof for nonlocality is constructed based on nonperfect correlations rather than constraints induced by stabilizers.

Moreover, since this quantum paradox is essentially a consequence of quantum nonlocality or contextuality, the features of quantum mechanics that do not exist in classical physics could lead to an operational advantage [7–9]. Thus one may design some tasks, such as some generalizations of the device-independent true random number generation protocol proposed in Ref. [45], using this quantum feature as a peculiar quantum resource.

ACKNOWLEDGMENTS

S.R. thanks Zheng-Hao Liu and Yihan Luo for helpful discussions in theory and experiment. This work at XJTU is supported by the National Nature Science Foundation of China (Grants No. 12074307, No. 11804271, and No. 91736104) and Ministry of Science and Technology of China (Grant No. 2016YFA0301404). This work at USTC is supported by the National Nature Science Foundation of China (Grants No. 11874345 and No. 11904357), and the Fundamental Research Funds for the Central Universities, USTC Tang Scholarship, Science and Technological Fund of Anhui Province for Outstanding Youth (Grant No. 2008085J02).

APPENDIX A: EXPERIMENTAL RESULTS OF $|S'\rangle$

Based on state $|S'\rangle$, we also can construct another Hardy-like quantum pigeonhole paradox. It needs to measure whether the following relations hold:

$$P(X_2X_3 = -1|Z_1 = +1) = 1, \quad (A1a)$$
$$P(X_1X_3 = +1|Z_2 = +1) = 1, \quad (A1b)$$
$$P(X_1X_2 = +1|Z_3 = +1) = 1, \quad (A1c)$$
$$P(Z_1 = Z_2 = Z_3 = +1) = \tfrac{1}{4}. \quad (A1d)$$

Similarly to $|S\rangle$ in the main text, we have measured Eqs. (A1a)–(A1d),

$$\langle X_2X_3\rangle = -0.921 \pm 0.011 \text{ if } Z_1 = +1, \quad (A2a)$$
$$\langle X_1X_3\rangle = +0.911 \pm 0.017 \text{ if } Z_2 = +1, \quad (A2b)$$
$$\langle X_1X_2\rangle = +0.923 \pm 0.008 \text{ if } Z_3 = +1, \quad (A2c)$$
$$P(Z_1 = Z_2 = Z_3 = +1) = 0.246 \pm 0.014. \quad (A2d)$$

In any local hidden variable theories or noncontextual hidden variable theories, according to the classical pigeonhole principle, events $X_2X_3 = -1$, $X_1X_3 = +1$ and $X_1X_2 = +1$ cannot jointly hold, which leads to a zero probability of obtaining $Z_1 = Z_2 = Z_3 = +1$. But our experimental results show a probability of 0.246 ± 0.014 to get $Z_1 = Z_2 = Z_3 = +1$. All these experimental results, including $|S\rangle$ and $|S'\rangle$, can discard the Hardy-like all-versus-nothing phenomenon, and successfully verify the Hardy-like quantum pigeonhole paradoxes.

APPENDIX B: THREE KINDS OF PCG STATES

Here we enumerate three kinds of general quantum states that can be used for the Hardy-like quantum pigeonhole paradox once again. The simplest quantum state $|S\rangle$ in each

category is consistent. The first kind of quantum state for the Hardy-like pigeonhole paradox is

$$|S_1(n)\rangle = \frac{1}{\sqrt{n+1}}\left[|\underbrace{0\cdots00}_{n}\rangle - |W;n,1\rangle\right], \tag{B1}$$

$$|W;n,k\rangle = |\underbrace{k\cdots kk}_{n-1}0\rangle + |\underbrace{k\cdots k}_{n-2}0k\rangle + \cdots + \cdots + |k0\underbrace{k\cdots k}_{n-2}\rangle + |0\underbrace{kk\cdots k}_{n-1}\rangle, \tag{B2}$$

where $n \geqslant 3$ and n is odd. Apart from quantum states $|S_1\rangle$, another two kinds of quantum states are n-qubits states and $(d+1)$-qudit states, which can be written as

$$|S_2\rangle = \frac{1}{\sqrt{1+C_n^2}}\left[|\underbrace{0\cdots00}_{n}\rangle - |\Phi\rangle\right], \tag{B3}$$

$$|S_3\rangle = \frac{1}{d}\left[|\underbrace{0\cdots00}_{d+1}\rangle - \sum_{l=1}^{d-1} e^{il\theta}|W;d+1,l\rangle\right], \tag{B4}$$

respectively. Here, $|\Phi\rangle = \sum_{\text{perm}} |00\underbrace{11\cdots11}_{n-2}\rangle$, where the summation is over all permutations of $|00\underbrace{11\cdots11}_{n-2}\rangle$, $n \geqslant 3$, and n is odd.

1. Multiqubit case 1

For quantum states $|S_1(n)\rangle$, we can have

$$\begin{aligned} X_2X_3\cdots X_n &= -1 \text{ if } Z_1 = 1,\\ X_1X_3\cdots X_n &= -1 \text{ if } Z_2 = 1,\\ &\cdots\\ X_1X_2\cdots X_{n-1} &= -1 \text{ if } Z_n = 1. \end{aligned} \tag{B5}$$

According to its classical assignment assumption in hidden variable theory (HVTs), X_l and Z_l can be assigned predefined values x_l and z_l, respectively, where $v = \pm 1$, $v \in \{z_l, x_l\}$. It follows that if the observables from one context (mutually commuting) satisfy a certain algebraic relationship, then the assigned predefined values obey the same algebraic constraint, i.e.,

$$\begin{aligned} x_2x_3\cdots x_n &= -1 \text{ if } z_1 = 1,\\ x_1x_3\cdots x_n &= -1 \text{ if } z_2 = 1,\\ &\cdots\\ x_1x_2\cdots x_{n-1} &= -1 \text{ if } z_n = 1. \end{aligned} \tag{B6}$$

Using the form of conditional event, these n events can be expressed as $\{x_2x_3\cdots x_n = -1|z_1 = +1\}$, $\{x_1x_3\cdots x_n = -1|z_2 = +1\}$, $\cdots$, and $\{x_1x_2\cdots x_{n-1} = -1|z_n = +1\}$. The probabilities of those n events are

$$\begin{aligned} &P_C(x_2x_3\cdots x_n = -1|z_1 = 1)\\ &\quad = P_C(x_1x_3\cdots x_n = -1|z_2 = 1)\\ &\quad = P_C(x_1x_2\cdots x_{n-1} = -1|z_n = 1) = 1, \end{aligned} \tag{B7}$$

in which we utilize subscript $C(Q)$ to denote classical (quantum) probability.

According to the probabilities being 1 of those n events, if event $z_1 = z_2 = \cdots = z_n = 1$ occurs, event $x_2x_3\cdots x_n = x_1x_3\cdots x_n = x_1x_2\cdots x_{n-1} = -1$ will also occur at the same time and be with the same probability, hence we can get

$$(x_1x_2\cdots x_{n-1}x_n)^n = -1. \tag{B8}$$

This method, multiplying both sides of the equations, usually can be used in the all-versus-nothing proof. But, obviously, $(x_1x_2\cdots x_{n-1}x_n)^{n-1}$ must be non-negative since all x_l are real numbers and $n-1$ is even. That is, the event $x_2x_3\cdots x_n = x_1x_3\cdots x_n = x_1x_2\cdots x_{n-1} = -1$ cannot occur via a classical assignment method. Therefore, it is logically appropriate that events $z_1 = z_2 = \cdots = z_n = 1$ and $x_2x_3\cdots x_n = x_1x_3\cdots x_n = x_1x_2\cdots x_{n-1} = -1$ occur simultaneously only when

$$P_C(z_1 = z_2 = \cdots = z_n = 1) = 0. \tag{B9}$$

On the other hand, the probability of classical event $z_1 = z_2 = \cdots = z_n = 1$ is equal to its quantum scenery,

$$P_Q(Z_1 = Z_2 = \cdots = Z_n = 1) = \frac{1}{n+1}. \tag{B10}$$

Equations (B9) and (B10) are contradictory. It is indicated that we cannot make classical assignments to observable values, and the hypothesis of HVTs is invalid. Therefore, for testing the paradox based on the quantum state $|S_1\rangle$, we only need to measure Eqs. (B5) and (B10).

If $n = 3$, the state is

$$|S_1(n=3)\rangle = (|000\rangle - |011\rangle - |101\rangle - |110\rangle)/2, \tag{B11}$$

which is the same as $|S\rangle$.

2. Multiqubit case 2

For quantum states $|S_2(n)\rangle$, we can have

$$X_mX_n = -1 \quad \text{if all} \quad Z_{j\neq m,n} = 1 \quad \text{and} \quad m \neq n. \tag{B12}$$

Similar to above, according to its classical assignment assumption in HVTs, its assigned predefined values obey the same algebraic constraint, i.e.,

$$x_mx_n = -1 \quad \text{if all} \quad z_{j\neq m,n} = 1 \quad \text{and} \quad m \neq n. \tag{B13}$$

Using the form of conditional event, the probabilities of these C_n^2 events are

$$\begin{aligned} &P_C(x_1x_2 = -1|z_3 = \cdots = z_n = 1)\\ &\quad = P_C(x_1x_3 = -1|z_2 = z_4\cdots = z_n = 1)\\ &\quad = P_C(x_{n-1}x_n|z_1 = z_2\cdots = z_n = 1) = 1. \end{aligned} \tag{B14}$$

Hence we can also get

$$(x_1x_2\cdots x_{n-1}x_n)^{n-1} = -1. \tag{B15}$$

But, obviously, $(x_1x_2\cdots x_{n-1}x_n)^{n-1}$ must be non-negative since all x_l are $+1$ or -1, and $n-1$ is even. Therefore, it is logically appropriate that events $z_1 = z_2 = \cdots = z_n = 1$ and $x_1x_2 = \cdots = x_1x_n = \cdots = x_{n-1}x_n = -1$ occur simultaneously only when

$$P_C(z_1 = z_2 = \cdots = z_n = 1) = 0. \tag{B16}$$

On the other hand, the probability of classical event $z_1 = z_2 = \cdots = z_n = 1$ is equal to its quantum scenery,

$$P_Q(Z_1 = Z_2 = \cdots = Z_n = 1) = \frac{2}{n(n-1)+2}. \quad \text{(B17)}$$

Equations (B16) and (B17) are contradictory. It is indicated that we cannot make classical assignments to observable values, and the hypothesis of HVTs is invalid. And, if $n = 3$, the state is

$$|S_2(n=3)\rangle = (|000\rangle - |011\rangle - |101\rangle - |110\rangle)/2, \quad \text{(B18)}$$

which is the same as $|S\rangle$.

3. Multiqudit case

The Pauli matrix group has applications in quantum computation, quantum teleportation, and other quantum protocols. This group is defined for a single qudit in the following manner:

$$Z_d = \sum_{n=0}^{d-1} e^{in\theta}|n\rangle\langle n|, \quad \text{(B19)}$$

$$X_d = \sum_{n=0}^{d-1} |n \oplus 1\rangle\langle n|, \quad \text{(B20)}$$

where $\theta = 2\pi/d$, $a \oplus b = (a+b) \bmod d$, and $XZ = ZXe^{i\theta}$. Furthermore, the Y gate can be written $Y = XZ$.

For quantum states $|S_3(n)\rangle$, we can have

$$\prod_{j=1, j\neq k}^{d+1} X_j = e^{-i\theta} \text{ if } Z_k = 1, \quad \text{(B21)}$$

where $k = 1, 2, \ldots, d+1$. According to its classical assignment assumption in HVTs, its assigned predefined values obey the same algebraic constraint, i.e.,

$$\prod_{j=1, j\neq k}^{d+1} x_j = e^{-i\theta} \text{ if } z_k = 1. \quad \text{(B22)}$$

Using the form of conditional event, the probabilities of these d events are

$$\begin{aligned} &P_C(x_2x_3\cdots x_{d+1} = e^{-i\theta}|z_1 = 1) \\ &\quad = P_C(x_1x_3\cdots x_{d+1} = e^{-i\theta}|z_2 = 1) \\ &\quad = P_C(x_1x_2\cdots x_d = e^{-i\theta}|z_{d+1} = 1) = 1. \end{aligned} \quad \text{(B23)}$$

According to the probabilities being 1 of those n events, if event $z_1 = z_2 = \cdots = z_d = z_{d+1} = 1$ occurs, event $x_2x_3\cdots x_{d+1} = x_1x_3\cdots x_{d+1} = \cdots = x_1x_2\cdots x_d = e^{-i\theta}$ will also occur at the same time and be with the same probability; hence we can get

$$(x_1x_2\cdots x_dx_{d+1})^d = e^{-id\theta} = -1. \quad \text{(B24)}$$

But, obviously, $(x_1x_2\cdots x_{n-1}x_n)^{n-1}$ must be non-negative. Therefore, it is logically appropriate that events $z_1 = z_2 = \cdots = z_d = z_{d+1} = 1$ and $x_2x_3\cdots x_{d+1} = x_1x_3\cdots x_{d+1} = \cdots = x_1x_2\cdots x_d = e^{-i\theta}$ occur simultaneously only when

$$P_C(z_1 = z_2 = \cdots = z_d = z_{d+1} = 1) = 0. \quad \text{(B25)}$$

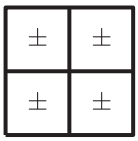

FIG. 5. A 2×2 quantum magic square occupied by a four-qubit quantum state.

On the other hand, the probability of classical event $z_1 = z_2 = \cdots = z_d = z_{d+1} = 1$ is equal to its quantum scenery,

$$P_Q(z_1 = z_2 = \cdots = z_d = z_{d+1} = 1) = \frac{1}{d^2}. \quad \text{(B26)}$$

Equations (B25) and (B26) are contradictory. It is indicated that we cannot make classical assignments to observable values, and the hypothesis of HVTs is invalid. And if $d = 2$, the state is

$$|S_3(d=2)\rangle = (|000\rangle - |011\rangle - |101\rangle - |110\rangle)/2, \quad \text{(B27)}$$

which is also the same as $|S\rangle$.

APPENDIX C: QUANTUM MAGIC SQUARE PARADOX

Putting 1 to n^2 ($n \geqslant 3$) in an $n \times n$ table such that the sum of the numbers in each row, column, and both diagonals are the same, one can get an nth-order magic square. A simplified version is the binary case in which only 0 and 1 are allowed to be filled, and such magic squares are called binary magic squares. Similar to the construction of PCGs, if mapping 0 and 1 to $X = 1$ and $X = -1$, respectively, one can build a kind of quantum magic square and the associated Hardy-like quantum magic square paradox.

We present a Hardy-like quantum magic square paradox based on a second-order quantum magic square as an example, seen in Fig. 5. Four qubits are put in the 2×2 magic square and labeled 1, 2, 3, and 4, from left to right and from top to bottom. As referred above, the predefined value of X_i on the ith qubit mapped to 0 or 1 can be considered as the associated binary number filled in the magic square.

Consider the state $|M\rangle = (|0000\rangle - |1100\rangle - |1010\rangle - |1001\rangle - |0110\rangle - |0101\rangle - |0011\rangle)/\sqrt{7}$. One can check that

$$P(X_3X_4 = -1|Z_1 = Z_2 = 1) = 1, \quad \text{(C1a)}$$

$$P(X_2X_4 = -1|Z_1 = Z_3 = 1) = 1, \quad \text{(C1b)}$$

$$P(X_2X_3 = -1|Z_1 = Z_4 = 1) = 1, \quad \text{(C1c)}$$

$$P(X_1X_4 = -1|Z_2 = Z_3 = 1) = 1, \quad \text{(C1d)}$$

$$P(X_1X_3 = -1|Z_2 = Z_4 = 1) = 1, \quad \text{(C1e)}$$

$$P(X_1X_2 = -1|Z_3 = Z_4 = 1) = 1, \quad \text{(C1f)}$$

$$P(Z_1 = Z_2 = Z_3 = Z_4 = 1) = \tfrac{1}{7}. \quad \text{(C1g)}$$

Therefore, if one measures Z_1 and Z_2 on qubits 1 and 2 and gets the outcomes of $Z_1 = 1$ and $Z_2 = 1$, one can infer that $X_3X_4 = -1$, and likewise the others. If $Z_1 = Z_2 = Z_3 = Z_4 = 1$ can jointly hold with a nonzero probability, then, in the classical framework, $X_1X_2 = X_1X_3 = X_1X_4 = X_2X_3 = X_2X_4 = X_3X_4 = -1$ is jointly held with a nonzero probability. Using a similar argument of the case of the three-qubit

Hardy-like quantum pigeonhole paradox, one can see that it is impossible. Then, we have constructed a Hardy-like quantum magic square paradox.

The following examples are more general Hardy-like quantum magic square paradoxes.

Example 1. Consider a (4×4)-qubit PCG state $|M(16)\rangle = \frac{1}{\sqrt{11}}(|\vec{0}\rangle_{\mathcal{S}} - \sum_{i=1}^{10} |\vec{1}\rangle_{\mathcal{S}_i}|\vec{0}\rangle_{\bar{\mathcal{S}}_i})$, where $\mathcal{S} = \{1, 2, \ldots, 16\}$ and $\{\mathcal{S}_i | i = 1, 2, \ldots, 10\} = \{\{4k+1, 4k+2, 4k+3, 4k+4\} | k = 0, 1, 2, 3\} \cup \{\{l, 4+l, 8+l, 12+l\} | l = 1, 2, 3, 4\} \cup \{1, 6, 11, 16\} \cup \{4, 7, 10, 13\}$. Assume that $|M(16)\rangle$ can be modeled by local hidden variable (LHV). Consider a run of the experiment for which $Z_1, Z_2, \ldots, Z_{16}$ are measured and the results $Z_1 = Z_2 = \cdots = Z_{16} = 1$ are obtained. Similar to the argument of the Hardy-like quantum pigeonhole (HLQP) paradox in the main text, one can finally conclude that $\prod_{j\in\mathcal{S}_1} X_j = \prod_{j\in\mathcal{S}_2} X_j = \cdots = \prod_{j\in\mathcal{S}_{10}} X_j = -1$. Based on that, one can find some solutions for $X_1, X_2, \ldots, X_{16}$. There is no contradiction.

Notice that $\prod_{i=1}^{10}(\prod_{j\in\mathcal{S}_i} X_j) = X_1X_4X_6X_7X_{10}X_{11}X_{13}X_{16} = 1$. We consider another PCG state, $|\tilde{M}(16)\rangle = \frac{1}{\sqrt{12}}(\sqrt{11}\,|M(16)\rangle - |1001011001101001\rangle)$. A new conditional constraint is as follows: If $Z_2 = Z_3 = Z_5 = Z_8 = Z_9 = Z_{12} = Z_{14} = Z_{15} = 1$ are obtained, then, necessarily, $X_1X_4X_6X_7X_{10}X_{11}X_{13}X_{16} = -1$. Next, we also consider a run of the experiment for which $Z_1, Z_2, \ldots, Z_{16}$ are measured and the results $Z_1 = Z_2 = \cdots = Z_{16} = 1$ are obtained. This extra constraint ensures that there is no consistent solution for $X_1, X_2, \ldots, X_{16}$ in the classical world according to the pigeonhole principle.

Let $m_r = (X_r + 1)/2$ be the number arranged in the rth grid of the binary magic square. Notice that $\prod_{j\in\mathcal{S}_i} X_j = (-1)^{\oplus_{j\in\mathcal{S}_i} m_j} = -1$ and

$$X_1X_4X_6X_7X_{10}X_{11}X_{13}X_{16} = (-1)^{m_1\oplus m_4\oplus m_6\oplus m_7\oplus m_{10}\oplus m_{11}\oplus m_{13}\oplus m_{16}} = -1, \tag{C2}$$

in which $\oplus$ stands for addition modulo 2 rather than modulo n. It follows that $\oplus_{j\in\mathcal{S}_1} m_j = \oplus_{j\in\mathcal{S}_2} m_j = \cdots = \oplus_{j\in\mathcal{S}_{10}} m_j = m_1 \oplus m_4 \oplus m_6 \oplus m_7 \oplus m_{10} \oplus m_{11} \oplus m_{13} \oplus m_{16} = 1$, a contradiction (the assumption of local realism can "induce" a binary magic square which is forbidden in the classical world). Then we can get a fourth-order conditional (with an extra constraint) Hardy-like quantum magic square paradox.

Remarks. Commonly, there are some prescribed constraints for a classical magic square (e.g., the 3×3 conventional magic square is arranged with numbers $1, 2, \ldots, 9$). Even for a binary magic square, usually the number of zeros (or ones) to be arranged should be prescribed (e.g., four zeros and five ones for a 3×3 binary magic square). However, for a quantum binary magic square, we would like to choose some other constraints, such as the extra constraint imposed in the above example. After all, our goal is just to show that a classically impossible magic square might be probabilistically produced if the associated quantum state admits a LHV model.

Example 2. Consider a nine-qubit PCG state, $|M(9)\rangle = \frac{1}{3}(|000000000\rangle - |111000000\rangle - |0001110000\rangle - |000000111\rangle - |100100100\rangle - |010010010\rangle - |001001001\rangle - |100010001\rangle - |001010100\rangle)$. Assume that $|M(9)\rangle$ can be modeled by LHV. Consider a run of the experiment for which $Z_1, Z_2, Z_3, Z_4, Z_5, Z_6, Z_7, Z_8, Z_9$ are measured and the results $Z_1 = Z_2 = Z_3 = Z_4 = Z_5 = Z_6 = Z_7 = Z_8 = Z_9 = 1$ are obtained. Likewise, one can conclude that the relations $X_1X_2X_3 = X_4X_5X_6 = X_7X_8X_9 = X_1X_4X_7 = X_2X_5X_8 = X_3X_6X_9 = X_1X_5X_9 = X_3X_5X_7 = -1$ should be satisfied. There is also no contradiction.

Notice that the product of these above eight relations gives rise to $X_1X_3X_7X_9 = 1$. One can use another PCG state, $|\tilde{M}(9)\rangle = \frac{1}{\sqrt{10}}(3|M(9)\rangle - |101000101\rangle)$, to construct a HLQP paradox. Likewise, consider a run of the experiment for which $Z_1, Z_2, Z_3, Z_4, Z_5, Z_6, Z_7, Z_8, Z_9$ are measured and the results $Z_1 = Z_2 = Z_3 = Z_4 = Z_5 = Z_6 = Z_7 = Z_8 = Z_9 = 1$ are obtained. In addition, $X_1X_2X_3 = X_4X_5X_6 = X_7X_8X_9 = X_1X_4X_7 = X_2X_5X_8 = X_3X_6X_9 = X_1X_5X_9 = X_3X_5X_7 = -1$, and one can get an extra relation $X_1X_3X_7X_9 = -1$. All such relations contradict the pigeonhole principle.

Let $m_k = (X_k + 1)/2$ be the number arranged in the kth grid of the binary magic square. One can get $m_1 \oplus m_2 \oplus m_3 = m_4 \oplus m_5 \oplus m_6 = m_7 \oplus m_8 \oplus m_9 = m_1 \oplus m_4 \oplus m_7 = m_2 \oplus m_5 \oplus m_8 = m_3 \oplus m_6 \oplus m_9 = m_1 \oplus m_5 \oplus m_9 = m_3 \oplus m_5 \oplus m_7 = 1$ and $m_1 \oplus m_3 \oplus m_7 \oplus m_9 = 1$, which cannot hold simultaneously in the classical world. This contradiction can induce another conditional Hardy-like quantum magic square paradox.

Example 3. We generalize the notion of binary magic square to the n-dimensional case. For example, a three-dimensional binary magic square of the order of 2 is an arrangement of k ones and $2^3 - k$ zeros in a $2 \times 2 \times 2$ cube, such that the XOR sum of the numbers in each edge, four main diagonals, and 12 other diagonals is the same. Here the XOR is the Exclusive OR logical gate that gives a true (1) output when the number of true inputs is odd.

Consider an eight-qubit PCG state, $|M(8)\rangle = \frac{1}{\sqrt{C_8^2+1}}(|00000000\rangle - \sum_{i=1}^{C_8^2} |11\rangle_{\mathcal{S}_i}|000000\rangle_{\bar{\mathcal{S}}_i})$, where $\mathcal{S}_i = \{a_i, b_i\}$ and $a_i \neq b_i \in \{1, 2, 3, \ldots, 8\}$. Also assume that $|M(8)\rangle$ can be modeled by LHV. Consider a run of the experiment for which $Z_1, Z_2, \ldots, Z_8$ are measured and the results $Z_1 = Z_2 = \cdots = Z_8 = 1$ are obtained. Likewise, one can finally conclude that $\prod_{j\in\mathcal{S}_1} X_j = \prod_{j\in\mathcal{S}_2} X_j = \cdots = \prod_{j\in\mathcal{S}_{28}} X_j = -1$, which contradict the pigeonhole principle.

Let $m_r = (X_r + 1)/2$. Notice that $\prod_{j\in\mathcal{S}_i} X_j = (-1)^{\oplus_{j\in\mathcal{S}_i} m_j} = -1$. Then one can get $\oplus_{j\in\mathcal{S}_1} m_j = \oplus_{j\in\mathcal{S}_2} m_j = \cdots = \oplus_{j\in\mathcal{S}_{28}} m_j = 1$, which is a contradiction. Namely, we get a generalized Hardy-like quantum magic square paradox.

APPENDIX D: AN EQUIVALENT HARDY'S PARADOX FOR THE THREE-QUBIT SCENARIO

First, let us consider a contextual version of Hardy's proof (the general Hardy's paradox and the three parties can even stay in the same place). Rewrite the state $|S\rangle$ as $|S\rangle = [|0\rangle_i(|00\rangle_{jk} - |11\rangle_{jk}) - |1\rangle_i(|01\rangle_{jk} + |10\rangle_{jk})]/2$. Let $U_{jk} = (I - X_jX_k)/2$, $D_i = (I + Z_i)/2$, and then one can get the Hardy conditions:

$$U_{23}U_{13}U_{12} = 0, \tag{D1a}$$

$$P(U_{23} = 1 | D_1 = 1) = 1, \tag{D1b}$$

$$P(U_{13} = 1|D_2 = 1) = 1, \quad \text{(D1c)}$$

$$P(U_{12} = 1|D_3 = 1) = 1, \quad \text{(D1d)}$$

$$P(D_1 = 1, D_2 = 1, D_3 = 1) = 1/4. \quad \text{(D1e)}$$

Similar to Ref. [14], we consider a run of the experiment in which D_1, D_2, D_3 are measured, and their outcomes $D_1 = 1, D_2 = 1, D_3 = 1$ are obtained, whose probability is $1/4$. Since we have $D_1 = 1$ in this run, one can infer from the above Hardy conditions that $U_{23} = 1$.

Assume that $|S\rangle$ admits a noncontextual hidden variable model; then the value of U_{23} is independent of the context. It is measured with an independent measurement choice on qubit 1. For this run, U_{23} determined by the hidden variables must be equal to 1, i.e., $U_{23}(\lambda) = 1$ (precisely, $[1 - (X_2X_3)(\lambda)]/2 = 1$). Likewise, one can infer that $U_{13}(\lambda) = 1$, and $U_{12}(\lambda) = 1$ holds in this run as well. Therefore, in this run, we have $U_{12}(\lambda)U_{13}(\lambda)U_{23}(\lambda) = 1$. If one consider the values of U_{12}, U_{13}, U_{23} in this run, one would have $U_{23}U_{13}U_{12} = 1$, which contradicts the Hardy condition ($U_{23}U_{13}U_{12} = 0$). Next, we put the three photons in different places and assume all the measurements performed on the photons are spacelike separated.

The above proof can be converted into a nonlocality version of the conventional Hardy's paradox. In this scenario, the system can be assumed to admit a LHV model rather than a noncontextual hidden variable model. As a consequence, for example, $U_{23}(\lambda) = [1 - (X2X3)(\lambda)]/2 = 1$ in the above proof will be replaced with $[1 - X_2(\lambda)X_3(\lambda)]/2 = 1$. The other arguments are similar. Precisely, the constraint $(I - X_2X_3)(I - X_1X_3)(I - X_1X_2)/8 = 0$ should be $(I - X_2X_3)(I - X_1X_3)(I - X_1X_2)/8 = 0$ in the proof of nonlocality. Moreover, constructing a Hardy-like quantum pigeonhole paradox also requires the assumption of local realism, but does not necessarily invoke $(I - X_2X_3)(I - X_1X_3)(I - X_1X_2)/8 = 0$. Instead, one can use the classical pigeonhole principle and Eqs. (2a)–(2d) to give a "sometimes" contradiction.

However, there is another type of Hardy's paradox, i.e., the version of the proof for contextuality. In that scenario, spacelike separated conditions for the measurement may not be satisfied. In a run of the experiment, the outcomes of (X_1X_2), (X_1X_3), and (X_2X_3) usually cannot be regarded as products of the outcomes of single operators X_1X_2, X_1X_3, and X_2X_3. Then one cannot construct a contradiction based on the classical pigeonhole principle. Besides such a contextual version of Hardy's proof, one can also get the contradiction by an inconsistent noncontextual value assignment, where $(X_1X_2)(X_2X_3) = X_1X_3$ implies $v(X_1X_2) * v(X_2X_3) = v(X_1X_3)$.

[1] H. J. Kimble, The quantum internet, Nature (London) **453**, 1023 (2008).

[2] C. Simon, Towards a global quantum network, Nat. Photon. **11**, 678 (2017).

[3] S. Wehner, D. Elkouss, and R. Hanson, Quantum internet: A vision for the road ahead, Science **362**, eaam9288 (2018).

[4] D. Gottesman, Theory of fault-tolerant quantum computation, Phys. Rev. A **57**, 127 (1998).

[5] S. Omkar, Y. S. Teo, and H. Jeong, Resource-Efficient Topological Fault-Tolerant Quantum Computation with Hybrid Entanglement of Light, Phys. Rev. Lett. **125**, 060501 (2020).

[6] V. Giovannetti, S. Lloyd, and L. Maccone, Advances in quantum metrology, Nat. Photon. **5**, 222 (2011).

[7] J. M. Matera, D. Egloff, N. Killoran, and M. B. Plenio, Coherent control of quantum systems as a resource theory, Quantum Sci. Technol. **1**, 01LT01 (2016).

[8] M. Hillery, Coherence as a resource in decision problems: The Deutsch-Jozsa algorithm and a variation, Phys. Rev. A **93**, 012111 (2016).

[9] T. Theurer, N. Killoran, D. Egloff, and M. B. Plenio, Resource Theory of Superposition, Phys. Rev. Lett. **119**, 230401 (2017).

[10] E. Chitambar and G. Gour, Quantum resource theories, Rev. Mod. Phys. **91**, 025001 (2019).

[11] J. S. Bell, On the Einstein-Podolsky-Rosen paradox, Phys. Phys. Fiz. **1**, 195 (1964).

[12] J. F. Clauser, M. A. Horne, A. Shimony, and R. A. Holt, Proposed Experiment to Test Local Hidden-Variable Theories, Phys. Rev. Lett. **23**, 880 (1969).

[13] D. M. Greenberger, M. A. Horne, and A. Zeilinger, Going beyond Bell's theorem, in *Bell's Theorem, Quantum Theory and Conceptions of the Universe*, edited by M. Kafatos (Springer, Dordrecht, 1989), pp. 69–72.

[14] L. Hardy, Nonlocality for Two Particles without Inequalities for Almost All Entangled States, Phys. Rev. Lett. **71**, 1665 (1993).

[15] A. Cabello, Nonlocality without inequalities has not been proved for maximally entangled states, Phys. Rev. A **61**, 022119 (2000).

[16] E. P. Specker, The Logic of Propositions Which are not Simultaneously Decidable, in *The Logico-Algebraic Approach to Quantum Mechanics*, edited by C. A. Hooker (Springer, Dordrecht, 1975), pp. 135–140.

[17] B.-H. Liu, X.-M. Hu, J.-S. Chen, Y.-F. Huang, Y.-J. Han, C.-F. Li, G.-C. Guo, and A. Cabello, Nonlocality from Local Contextuality, Phys. Rev. Lett. **117**, 220402 (2016).

[18] X.-M. Hu, J.-S. Chen, B.-H. Liu, Y. Guo, Y.-F. Huang, Z.-Q. Zhou, Y.-J. Han, C.-F. Li, and G.-C. Guo, Experimental Test of Compatibility-Loophole-Free Contextuality with Spatially Separated Entangled Qutrits, Phys. Rev. Lett. **117**, 170403 (2016).

[19] W. Tang and S. Yu, Construction of state-independent proofs for quantum contextuality, Phys. Rev. A **96**, 062126 (2017).

[20] D. Qu, K. Wang, L. Xiao, X. Zhan, and P. Xue, State-independent test of quantum contextuality with either single photons or coherent light, npj Quantum Inf. **7**, 154 (2021).

[21] W.-R. Qi, J. Zhou, L.-J. Kong, Z.-P. Xu, H.-X. Meng, R. Liu, Z.-X. Wang, C. Tu, Y. Li, A. Cabello *et al.*, Stronger Hardy-like proof of quantum contextuality, Photon. Rese. **10**, 1582 (2022).

[22] Y. Aharonov, S. Nussinov, S. Popescu, and L. Vaidman, Peculiar features of entangled states with postselection, Phys. Rev. A **87**, 014105 (2013).

[23] Y. Aharonov, F. Colombo, S. Popescu, I. Sabadini, D. C. Struppa, and J. Tollaksen, Quantum violation of the pigeonhole principle and the nature of quantum correlations, Proc. Natl. Acad. Sci. USA **113**, 532 (2016).

[24] Z.-H. Liu, W.-W. Pan, X.-Y. Xu, M. Yang, J. Zhou, Z.-Y. Luo, K. Sun, J.-L. Chen, J.-S. Xu, C.-F. Li, and G.-C. Guo, Experimental exchange of grins between quantum Cheshire cats, Nat. Commun. **11**, 3006 (2020).

[25] M.-C. Chen, C. Liu, Y.-H. Luo, H.-L. Huang, B.-Y. Wang, X.-L. Wang, L. Li, N.-L. Liu, C.-Y. Lu, and J.-W. Pan, Experimental demonstration of quantum pigeonhole paradox, Proc. Natl. Acad. Sci. USA **116**, 1549 (2019).

[26] M. Waegell, T. Denkmayr, H. Geppert, D. Ebner, T. Jenke, Y. Hasegawa, S. Sponar, J. Dressel, and J. Tollaksen, Confined contextuality in neutron interferometry: Observing the quantum pigeonhole effect, Phys. Rev. A **96**, 052131 (2017).

[27] S. Yu and C. Oh, Quantum pigeonhole effect, Cheshire cat and contextuality, arXiv:1408.2477.

[28] M. S. Leifer and R. W. Spekkens, Pre- and Post-Selection Paradoxes and Contextuality in Quantum Mechanics, Phys. Rev. Lett. **95**, 200405 (2005).

[29] J. Tollaksen, Pre-and post-selection, weak values and contextuality, J. Phys. A: Math. Theor. **40**, 9033 (2007).

[30] W. Tang, S. Yu, and C. H. Oh, Greenberger-Horne-Zeilinger Paradoxes from Qudit Graph States, Phys. Rev. Lett. **110**, 100403 (2013).

[31] Z.-H. Liu, J. Zhou, H.-X. Meng, M. Yang, Q. Li, Y. Meng, H.-Y. Su, J.-L. Chen, K. Sun, J.-S. Xu, C.-F. Li, and G.-C. Guo, Experimental test of the Greenberger-Horne-Zeilinger-type paradoxes in and beyond graph states, NPJ Quantum Inf. **7**, 66 (2021).

[32] N. E. Bonesteel, L. Hormozi, G. Zikos, and S. H. Simon, Braid Topologies for Quantum Computation, Phys. Rev. Lett. **95**, 140503 (2005).

[33] D. S. Hall, M. W. Ray, K. Tiurev, E. Ruokokoski, A. H. Gheorghe, and M. Möttönen, Tying quantum knots, Nat. Phys. **12**, 478 (2016).

[34] D. Chruscinski and A. Jamiolkowski, *Geometric Phases in Classical and Quantum Mechanics* (Springer, Birkhäuser Boston, MA, 2012), Vol. 36.

[35] S. Bravyi and A. Kitaev, Universal quantum computation with ideal Clifford gates and noisy ancillas, Phys. Rev. A **71**, 022316 (2005).

[36] S. Kochen and E. P. Specker, The problem of hidden variables in quantum mechanics, in *The Logico-algebraic Approach to Quantum Mechanics*, edited by C. A. Hooker (Springer, Dordrecht, 1975), pp. 293–328.

[37] A. Peres, Two simple proofs of the Kochen-Specker theorem, J. Phys. A: Math. Gen. **24**, L175 (1991).

[38] A. Cabello, J. Estebaranz, and G. García-Alcaine, Bell-Kochen-Specker theorem: A proof with 18 vectors, Phys. Lett. A **212**, 183 (1996).

[39] W. Tang, Hardy-like quantum pigeonhole paradox and the projected-coloring graph state, Phys. Rev. A **105**, 032457 (2022).

[40] L. S. Penrose and R. Penrose, Impossible objects: A special type of visual illusion, Brit. J. Psyc. **49**, 31 (1958).

[41] L. Hardy, Quantum Mechanics, Local Realistic Theories, and Lorentz-Invariant Realistic Theories, Phys. Rev. Lett. **68**, 2981 (1992).

[42] S.-H. Jiang, Z.-P. Xu, H.-Y. Su, A. K. Pati, and J.-L. Chen, Generalized Hardy's Paradox, Phys. Rev. Lett. **120**, 050403 (2018).

[43] Y.-H. Luo, H.-Y. Su, H.-L. Huang, X.-L. Wang, T. Yang, L. Li, N.-L. Liu, J.-L. Chen, C.-Y. Lu, and J.-W. Pan, Experimental test of generalized Hardy's paradox, Sci. Bull. **63**, 1611 (2018).

[44] N. D. Mermin, Quantum mysteries refined, Am. J. Phys. **62**, 880 (1994).

[45] H.-W. Li, M. Pawłowski, R. Rahaman, G.-C. Guo, and Z.-F. Han, Device- and semi-device-independent random numbers based on noninequality paradox, Phys. Rev. A **92**, 022327 (2015).

[46] R. Ramanathan, M. Horodecki, H. Anwer, S. Pironio, K. Horodecki, M. Grnfeld, S. Muhammad, M. Bourennane, and P. Horodecki, Practical no-signalling proof randomness amplification using hardy paradoxes and its experimental implementation, arXiv:1810.11648.

[47] V. Potoček, F. M. Miatto, M. Mirhosseini, O. S. Magaña-Loaiza, A. C. Liapis, D. K. L. Oi, R. W. Boyd, and J. Jeffers, Quantum Hilbert Hotel, Phys. Rev. Lett. **115**, 160505 (2015).

[48] L. Heaney, A. Cabello, M. F. Santos, and V. Vedral, Extreme nonlocality with one photon, New J. Phys. **13**, 053054 (2011).

[49] M. Gachechiladze, C. Budroni, and O. Gühne, Extreme Violation of Local Realism in Quantum Hypergraph States, Phys. Rev. Lett. **116**, 070401 (2016).

[50] C. Zhang, Y.-F. Huang, Z. Wang, B.-H. Liu, C.-F. Li, and G.-C. Guo, Experimental Greenberger-Horne-Zeilinger-Type Six-Photon Quantum Nonlocality, Phys. Rev. Lett. **115**, 260402 (2015).

[51] C. Sabín and G. García-Alcaine, A classification of entanglement in three-qubit systems, Eur. Phys. J. D **48**, 435 (2008).